electronics

Article

Research of the Oscillation Start-Up Time in an Extended Interaction Oscillator Driven by a Pseudospark-Sourced Sheet Electron Beam

Ruibin Peng, Hailong Li *, Yong Yin, Xiaotao Xu, Qingyun Chen, Liangjie Bi, Che Xu, Bin Wang, Xuesong Yuan, Ping Zhang and Lin Meng

The Terahertz Science and Technology Key Laboratory of Sichuan Province, School of Electronic Science and Engineering, University of Electronic Science and Technology of China, Chengdu 610054, China; 201711040130@std.uestc.edu.cn (R.P.); yinyong@uestc.edu.cn (Y.Y.); xxt@std.uestc.edu.cn (X.X.); cqy@std.uestc.edu.cn (Q.C.); biliangjie1990@gmail.com (L.B.); chexu1992@163.com (C.X.); wb@uestc.edu.cn (B.W.); yuanxs@uestc.edu.cn (X.Y.); zhangping@uestc.edu.cn (P.Z.); meng@uestc.edu.cn (L.M.)

* Correspondence: lihailong@uestc.edu.cn

Abstract: High current density and high brightness are critical factors for high-power and compact extended interaction oscillators (EIOs) which are operated in the terahertz (THz) waveband. The pseudospark-sourced (PS) sheet electron beam, which combines merits including high current density, a relatively big beam cross-section and no requirement for the external focusing magnetic field, is a good choice for application to high-frequency EIO. The pulse generated by the PS electron beam can last around tens of nanoseconds or even less, thus the EIO's oscillation start-up time (OST) should be short enough. This paper researched how to reduce OST in an EIO driven by the PS sheet electron beam. The authors realized that the OST of EIO was very sensitive to the gap length under the equal period. The distribution of the electric field is optimized by adjusting the length of the gap. The strong electric field strength is conducive to the beam-wave interaction, and the OST is affected by the beam-wave interaction. When the gap length reaches a suitable value, the OST becomes the shortest. The simulation results showed the EIO's shortest OST was 8 ns and the corresponding peak output power was 2 kW at 0.19 THz, while the current density was 500 A/cm^2. When current density reached 10,000 A/cm^2, the shortest OST could even be 1.9 ns.

Keywords: extended interaction oscillator (EIO); pseudospark-sourced (PS) electron beam; oscillation start-up time (OST); gap length; conductivity; efficiency; terahertz (THz)

check for updates

Citation: Peng, R.; Li, H.; Yin, Y.; Xu, X.; Chen, Q.; Bi, L.; Xu, C.; Wang, B.; Yuan, X.; Zhang, P.; et al. Research of the Oscillation Start-Up Time in an Extended Interaction Oscillator Driven by a Pseudospark-Sourced Sheet Electron Beam. *Electronics* **2022**, *11*, 664. https://doi.org/10.3390/electronics11040664

Academic Editor: Yahya M. Meziani

Received: 10 January 2022
Accepted: 18 February 2022
Published: 21 February 2022

1. Introduction

The millimeter-wave (MMW) and terahertz-wave radiation sources have a lot of useful applications, including biological spectroscopy, molecular spectroscopy, high data rate communications, security checks and material research [1–3]. Among these broad applications, the broadband and lightweight source of high-power THz radiation are vital to communication radars, high-resolution imaging and high data rate communications. Vacuum electronic devices (VEDs) [4] have the superiority of robustness and high output power, compared with solid-state semiconductor devices. Because of the high-power output, the VEDs have many applications in MMW, even in the THz region. The compact and high-power sources at THz are rare and are needed for many vital projects. The extended interaction klystrons (EIKs) and the EIOs [5] have been regarded as attractive sources to satisfy these applications because they combine the klystrons' ability to have a high power and the traveling wave tubes' characteristic of wide bandwidth [6]. The EIOs have a compact configuration and high-power output [7]. The EIOs at THz are in urgent need of power which is precisely focused and has a high current density electron beam.

For a conventional thermionic cathode system, the electron transmission in the beam tunnel needs the external magnetic field [8] and it is a challenge to augment the current density for the conventional thermionic cathode system [9]. However, some experimental results demonstrated that hundreds of amperes of electron beam generated by the PS electron source can also be transmitted in the absence of an external guiding magnetic field [10]. The PS electron beam's current density can even achieve 10^4 A/cm^2 [11]. The PS electron beam has many noble advantages, such as a compact structure, high beam current density, low vacuum environment and no requirement for the external focusing magnetic field [12–15]. The PS electron beam uses a cold cathode, which makes it have a longer life and is more durable and reliable [16]. Compared with the conventional thermionic cathode electron gun, it is a better choice to use the PS electron beam to produce millimeter and THz waves. Because of a short PS electron beam pulse duration (generally about tens of nanoseconds or even less), the OST of EIO using the PS electron beam should be as short as possible. In general, the EIO's OST needs to reach around tens of nanoseconds or even shorter. Whether the PS electron beam EIO works, its OST is a key factor [17].

In the paper, the authors present an original report of the preliminary design of a G-band EIO using the PS sheet electron beam, and the authors studied and simulated how to shorten the OST of the EIO. This research combines the PS electron beam's advantage of a high current density and the sheet beam's superiority of a large cross-sectional area to produce high-power millimeter-wave radiation [10,18]. This method is a suitable solution to generate high-frequency and high-power millimeter-wave, or even terahertz-wave radiation sources. The PS sheet electron beam's characteristics were researched to adapt the EIO. At the same time, EIO's OST should be short enough to meet the requirement of the PS electron beam. Section 2 gives a brief introduction of the PS electron source's feature and optimization of a G-band EIO. Section 3 shows the simulation of the G-band EIO with the PS sheet electron beam. Section 4 researches the influence of the gap length and conductivity of background materials on the OST of an EIO. Section 5 is the conclusions and discussions.

2. Characteristics of the EIO Driven by PS Electron Source

When the microwave devices are operated in the THz region, a quite high electron beam current density is essential. The PS electron resources become a viable and attractive choice for THz radiation sources [19]. The PS discharge is a type of gas discharge, which is characterized by axial symmetry, short duration and relatively low air pressure. The PS discharge can generate a fairly high current density (up to 10^8 A/m^2), rapid current rising speed (up to 10^{12} A/s) and nanosecond-level electron beam pulse [20–22]. When the PS discharge process begins, the original high-energy electrons are emitted from the anode to the interaction circuit. The background gas is ionized by the electron beam with high-energy in the drift tube and it forms a plasma channel. Because of the repulsive force between the electrons, the following electrons from the PS discharge repel the plasma electrons. The ions remain stable because they are relatively heavier than electronics. Thus, the generated cation channel plays the role of focusing and guiding the PS electron beam. The size and shape of the electron emission hole can transform the cross-section of the electron beam. Compared to the conventional thermionic cathode system, the PS electron source used to drive THz EIO has some advantages, which contain high power, and inexpensive and compact features.

Figure 1 shows a PS electron source experimental device. The PS discharge system includes a hollow cathode, some intermediate electrodes, some insulators and an anode with a rectangular hole. The DC power source and the hollow cathode are connected by a charging resistor. The PS electrons are emitted from the five-gap PS discharge cavity. When the anode voltage is zero, the hollow cathode is connected to a quite considerable negative voltage and the gas pressure in the device is at an appropriately low value. At the same time, the working gas (e.g., nitrogen, argon, hydrogen, xenon, etc.) is slowly injected into the device from the anode side. It is not necessary to use an external guide magnetic field.

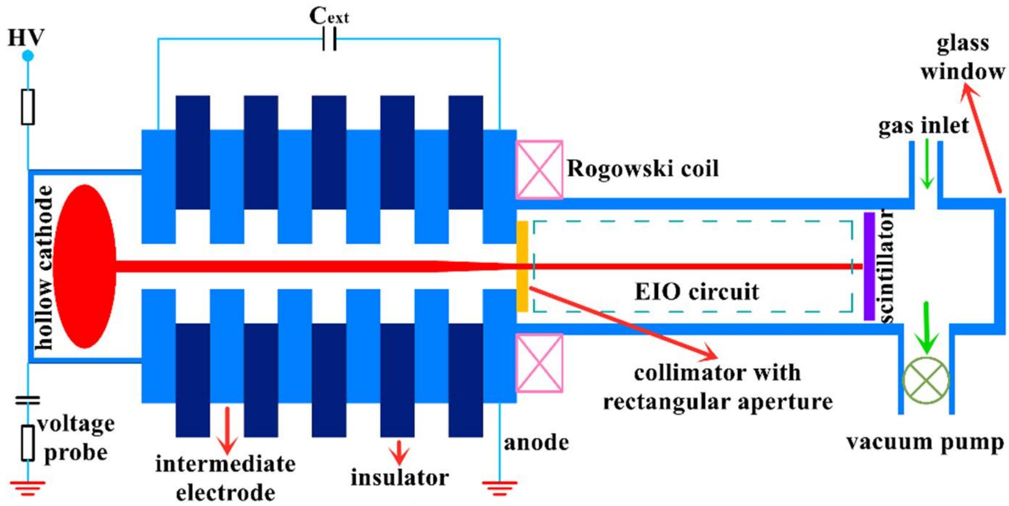

Figure 1. A PS electron source experimental device.

The electron beam pulse depicted in Figure 2 [7] was verified experimentally in the absence of the focusing magnetic field. It is a key point that the PS electron beam EIO's OST should be short enough because it can be seen in Figure 2 that the PS electron beam's pulse duration is only about tens of nanoseconds. In general, the EIO's OST needs to be reduced to around tens of nanoseconds or less. Whether the PS electron beam EIO works, the EIO's OST is very critical.

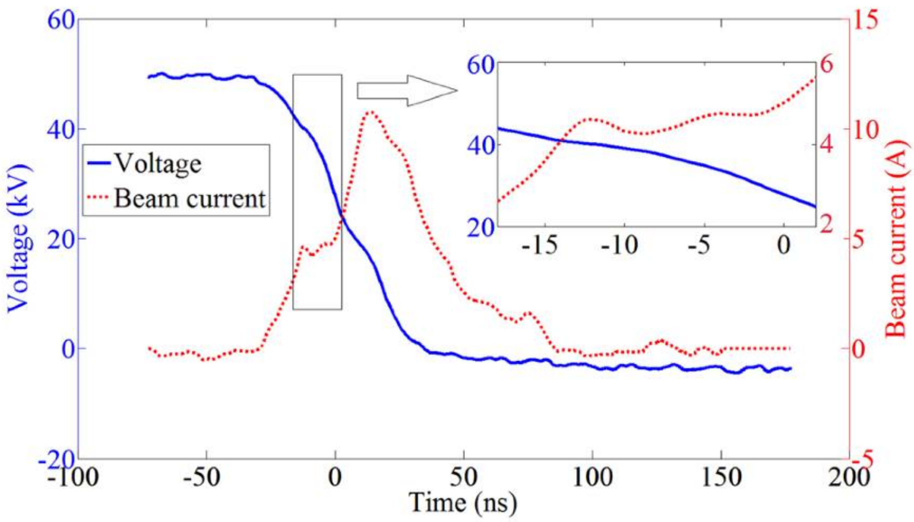

Figure 2. The voltage curve and current curve produced by PS discharge over time.

Figure 3 is the structure of the designed EIO. An output waveguide and a resonant slow-wave structure make up the interaction circuit. The slow-wave structure includes nine gaps, a sheet beam tunnel, and two identical coupling cavities. The multi-gap slow-wave structure is intersected with a 0.7 mm $\times$ 0.25 mm rectangular electron beam tunnel. Two identical coupling cavities are symmetrically distributed above and below. The electromagnetic wave produced by the EIO in the resonant slow-wave structure is transmitted to the output structure. There is a coupling hole between the resonant slow-wave structure and the standard output waveguide. Table 1 is a list of the detailed device dimensions. The gap length of the EIO is ranged from 0.1 mm to 0.29 mm, searching for the shortest OST.

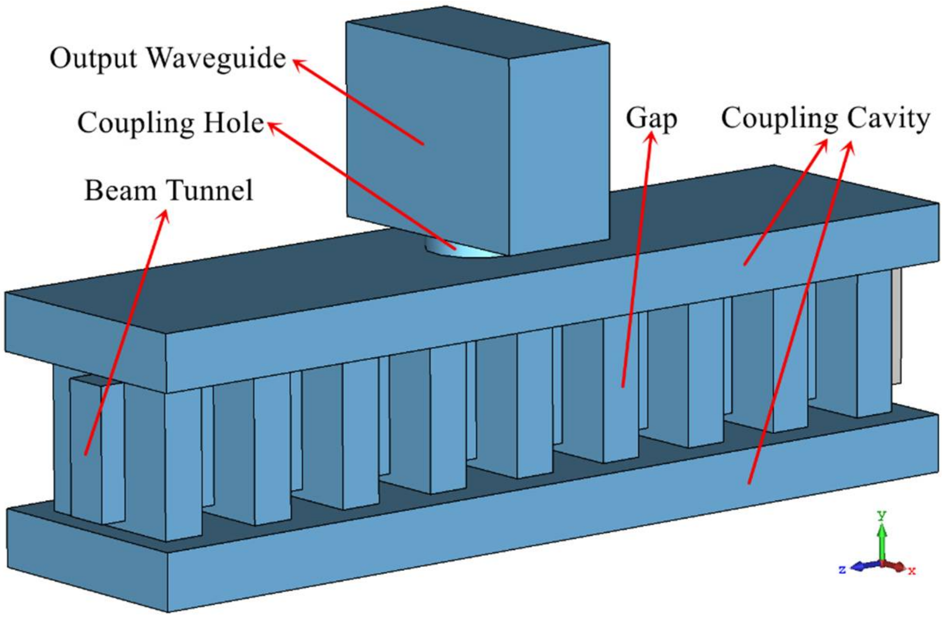

Figure 3. Structure of the designed THz EIO circuit.

Table 1. EIO dimensions.

Symbol	Quantity	Dimension (mm)
C_x	Cavity width	1.3
C_y	Cavity height	0.3
C_Z	Cavity length	5
G_X	Gap width	0.9
G_Y	Gap height	0.8
G_Z	Gap length	0.1~0.29
P	Period	0.56
R	Coupling hole radius	0.27
	Beam tunnel	0.7 × 0.25

3. Simulation of the G-Band PS Sheet Electron Beam EIO

Figure 4 illustrates the dispersion curves of the EIO with different gap lengths. The intersections of the electron beam lines and the dispersion curves are the operating frequencies. The electron beam velocity could be calculated from the electron beam voltage. The time interval for electrons to move from a slot to the neighboring one is the same as the electromagnetic wave's period, which is determined by the interaction circuit. In this situation, a high-efficiency interaction between the slow-wave structure and the high-energy electrons will be realized, so the high output power can be obtained.

Research of the EIO's characteristics and improving its performance is achieved by using the CST Particle Studio. In these simulations, the electron source is a DC electron beam with a voltage of 44 kV. The current density was set to 500 A/cm^2 and the corresponding total beam current was 875 mA, having considered the loss of electrons because of a high interception rate (beam current density >10^8 A/m^2 can be achieved theoretically). The conductivity of the background material was 5.9×10^7 S/m. The axial magnetic field used to focus was 1.5 T. When the synchronous condition was satisfied, the simulations showed that the oscillation could happen and that the output waveguide could generate power.

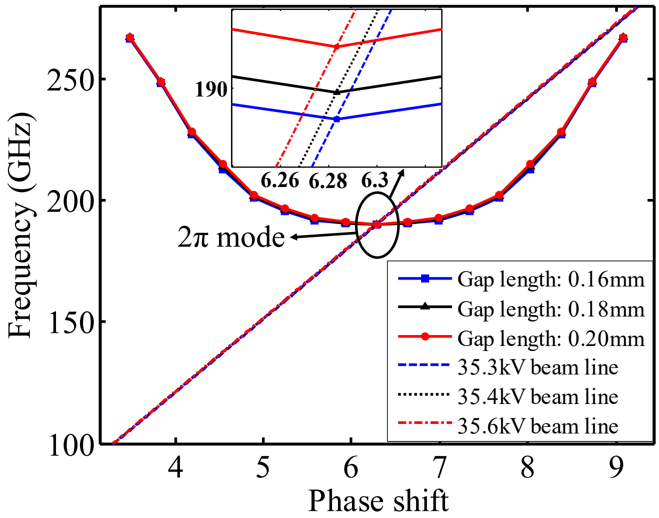

Figure 4. Dispersion curves of the EIO circuit with different gap lengths.

The oscillation gradually stabilizes after 8 ns of the DC beam injection into the interaction circuit. Figure 5 is the normalized electric field strength in the Z and Y directions, and the oscillated contour plots of electric field strength on the Z-Y and Y-X cut planes. The upper two graphs in Figure 5 are the normalized electric field intensity on the central axis of the electron beam channel and the normalized electric field intensity on the central axis of the coupling hole. The electric field intensity in the Z-direction at the middle point is the strongest, so the output power can be well emitted from the output waveguide, which is at the mid-point of the top coupling cavity.

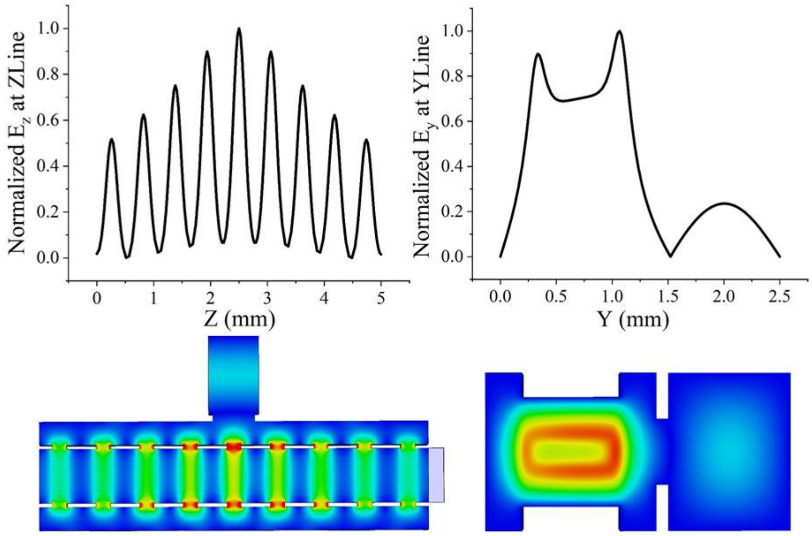

Figure 5. The normalized electric field intensity in the Z-direction and Y-direction and the oscillated contour plots of electric field strength on the Z-Y and Y-X cut planes.

The trajectory of electrons in the beam tunnel on the Z-Y cross-section is shown in the upper part of Figure 6. The bottom part of Figure 6 is the phase space plots of electrons. During the velocity modulation period, the quicker electrons catch up with the slower electrons to exchange energy, resulting in the periodic electron density modulation. At the same time, part of the energy in the electrons will also be transferred to the electromagnetic field.

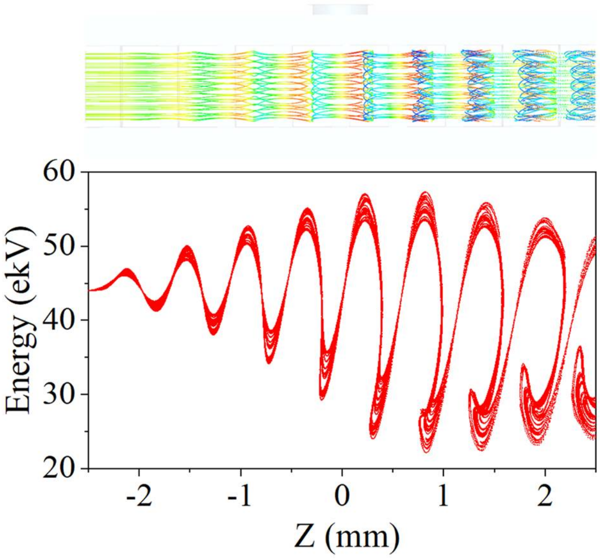

Figure 6. The trajectory of electrons on the Z-Y cross-section and the phase space plots of electrons.

The pulse duration of the PS-sourced electron source is relatively short, generally on the order of tens of nanoseconds, so the OST should be as short as possible to meet the requirement of the PS electron beams. Figure 7 is a stable output signal lasting 100 ns and the output power is 2 kW. The OST is approximately 8 ns. Quite a short time meets the need for rapid oscillation. The inner part of Figure 7 is the frequency spectrum, from which it can be seen that the main frequency is at 189.52 GHz.

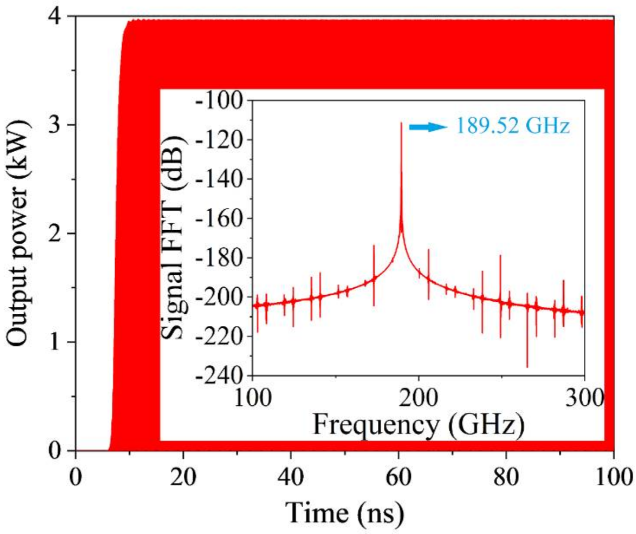

Figure 7. Output power and the corresponding frequency spectrum (inset).

4. The Effect of Gap Length and Conductivity of Background Materials on OST

When the beam current density is 500 A/cm^2, the change trends of the EIOs' OST with voltage are shown in Figure 8a. The EIO's gap lengths are respectively set as 0.16 mm, 0.18 mm and 0.2 mm. As the voltage is enlarged, the OST first decreases and then increases. When the beam voltage is around 43.5 kV or 44 kV, the OST is the shortest of all. The 0.18 mm gap length achieves a shorter OST than other gap lengths. Figure 8b displays the impact of gap length on the shortest OST and the corresponding efficiency. The shortest OST first decreases and then increases with the enlarging gap. When gap length reaches 0.18 mm, the OST is the shortest (8 ns) and the efficiency is 5.1%. The OST of 8 ns meets the requirement of the PS electron beam. To sum up, the shortest OST could be realized by adjusting the appropriate gap length.

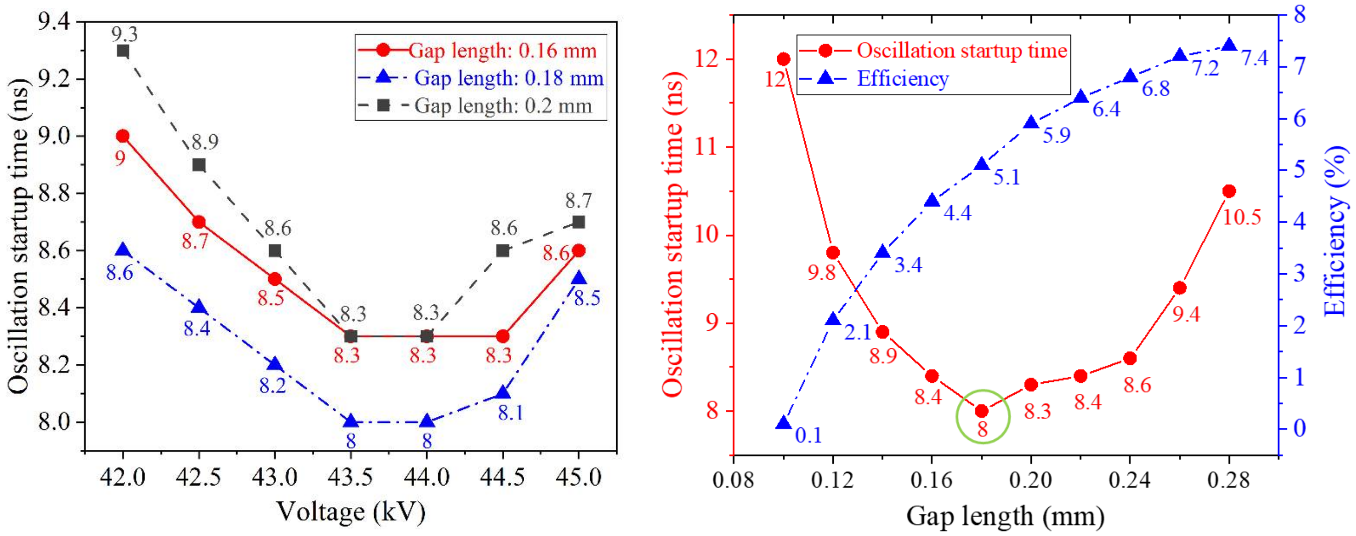

(**a**) (**b**)

Figure 8. (**a**) The change trends of the EIO's OST with the voltage (three various gap lengths); (**b**) The impact of the gap length on the shortest OST and the efficiency.

Field E_Z along the beam tunnel with different gap lengths is plotted in Figure 9. When the gap length is different, the field strength also changes. The distribution of the electric field is optimized by adjusting the length of the gap. Electrons in the gaps are modulated by the positive half-cycle of the sinusoidal electric field. When the gap length is 0.18 mm, the peak value of the electric field strength is the strongest in each gap (except for the two furthest gaps). The output hole is set in the center of the cavity. The strong electric field strength is conducive to the beam-wave interaction. The beam-wave interaction meanwhile plays a crucial role in shortening the OST, so OST reaches the shortest of all while gap length is 0.18 mm.

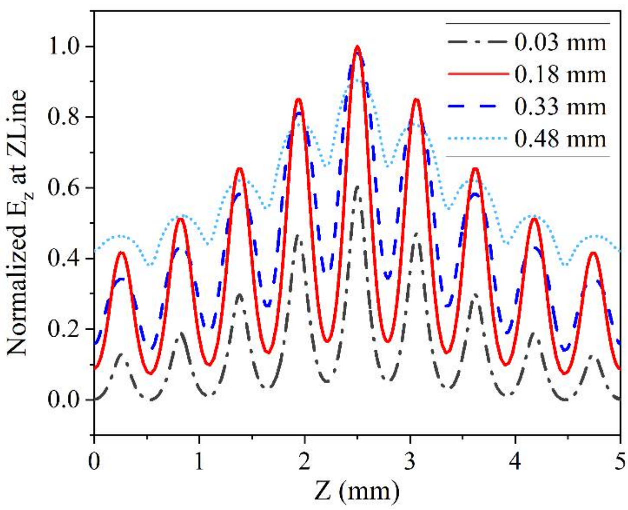

Figure 9. Field E_Z along the beam tunnel with different gap lengths.

However, the output power will decrease drastically as the frequency increases, because of the large power loss in the copper circuits. Figure 10a illustrates the shortest OST versus gap length in different conductivity materials. The higher the conductivity is, the shorter the OST is. When conductivity material is different, the gap length corresponding to the shortest OST changes. The PS electron beam EIO's gap length should be designed according to its material's conductivity in order to achieve the shortest OST.

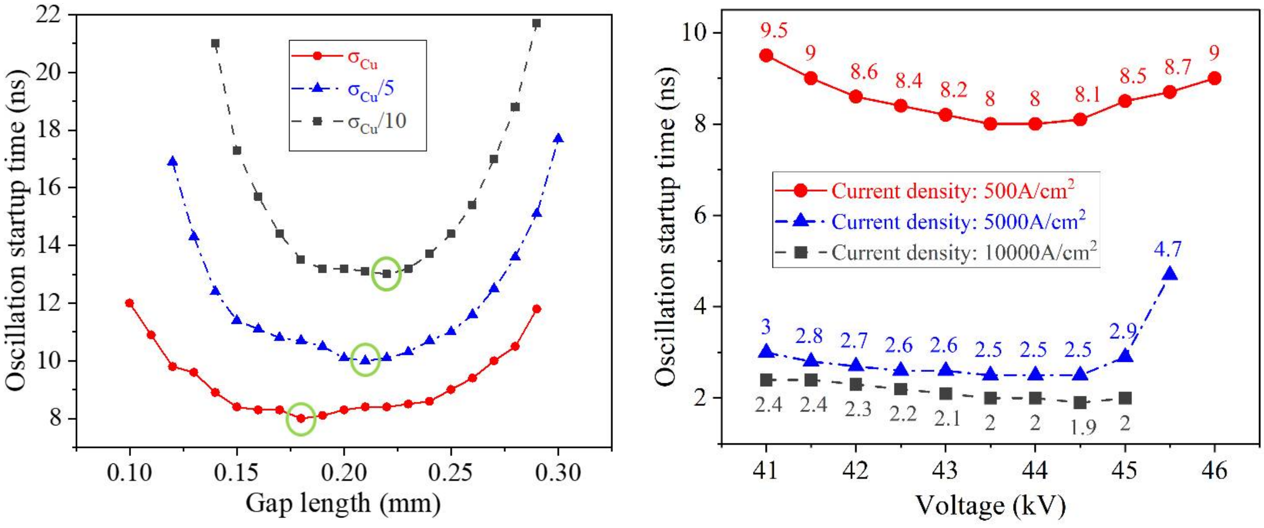

(**a**) (**b**)

Figure 10. (**a**) The shortest OST versus gap length for different conductivity materials; (**b**) The variation trend of the shortest OST with voltage at different current densities.

Figure 10b shows the variation trend of the shortest OST with the voltage at different current densities. When the current density is 5000 A/cm^2 and even 10,000 A/cm^2, the shortest OST can be around 2 ns. When the current density is large enough, a very short OST can be achieved. However, the high current density increases the space charge effect, so the repulsive force between electrons becomes strong, which reduces the electron bunching. As the current density increases, the maximum operating voltage of EIO gradually decreases, as shown in the right part of Figure 10b. The OST of EIOs in other reported research papers is listed in Table 2.

Table 2. The OST of different EIOs.

Extended Interaction Oscillators	OST
0.19 THz pencil beam EIO [7]	7.3 ns
0.2 THz sheet beam EIO [18]	5.1 ns
0.35 THz sheet beam EIO [9]	4.3 ns
The EIO in this paper	1.9 ns

5. Conclusions and Discussions

This paper achieves a sheet electron beam G-band EIO, which has short OST. The EIO simulations give promising results, which include that the OST is 8 ns, the output power is 2 kW and the corresponding efficiency is 5.1% at 189 GHz (using 44 kV voltage and 500 A/cm^2 current density PS discharging). The authors found that the shortest OST could be realized by adjusting the appropriate gap length. The authors achieved the purpose of optimizing the electric field distribution by adjusting the length of the gap. When the gap length is 0.18 mm, the peak value of the electric field strength is the strongest in almost every gap. The strong electric field strength is conducive to the beam-wave interaction. The beam-wave interaction meanwhile plays a key role in shortening the OST, so OST reaches the shortest of all while gap length is 0.18 mm. The shortest OST is 8 ns. When the material conductivity is changed, the gap length of the shortest OST is also different. The PS electron beam EIO gap length should be designed according to its material's conductivity in order to achieve rapid oscillation. When the current density is 5000 A/cm^2 and even 10,000 A/cm^2, the shortest OST can be around 2 ns, which is much shorter than the duration of the PS pulse. In the future, the designed EIO will be manufactured in the experiments to verify whether it is the same as the simulation results.

Author Contributions: Conceptualization, R.P. and Y.Y.; methodology, L.B. and C.X.; software, R.P. and X.X.; formal analysis, H.L.; investigation, R.P. and Y.Y.; data curation, X.X. and Q.C.; writing—original draft preparation, R.P.; writing—review and editing, H.L. and B.W.; visualization, X.Y. and P.Z.; supervision, Y.Y. and L.M.; project administration, B.W. and L.M. All authors have read and agreed to the published version of the manuscript.

Funding: This research was funded by the National Natural Science Foundation of China (Grant Nos. 61671116, 61771096 and 11905026), the National Key Research and Development Program of China (Grant No. 2019YFA0210202) and the Fundamental Research Funds for the Central Universities (Grant Nos. ZYGX2019Z006 and ZYGX2019J012).

Institutional Review Board Statement: Not applicable.

Informed Consent Statement: Not applicable.

Data Availability Statement: Not applicable.

Conflicts of Interest: The authors declare no conflict of interest.

References

1. Liu, W.; Zhang, Z.; Zhao, C.; Guo, X.; Liao, S. Design and simulation of a sub-terahertz folded-waveguide extended interaction oscillator. *Phys. Plasmas* **2017**, *24*, 063106. [CrossRef]
2. Zhang, Z.; Yin, Y.; Bi, L.J.; Chang, Z.W.; Xu, C.P.; Wang, B.; Meng, L. The effect of velocity spread of pseudospark-sourced electron beam to Y-band extended interaction oscillator. *Phys. Plasmas* **2017**, *24*, 043103. [CrossRef]
3. Siegel, P.H. Terahertz technology. *IEEE Trans. Microw. Theory Tech.* **2002**, *50*, 910–928. [CrossRef]
4. Booske, J.H.; Dobbs, R.J.; Joye, C.D.; Kory, C.L.; Neil, G.R.; Park, G.S.; Park, J.; Temkin, R.J. Vacuum Electronic High Power Terahertz Sources. *IEEE Trans. Terahertz Sci. Technol.* **2011**, *1*, 54–75. [CrossRef]
5. Zhang, K.; Wu, Z.; Liu, S. Study of An Extended Interaction Oscillator with A Rectangular Reentrance Coupled-cavity in Terahertz Region. *J. Infrared Millim. Terahertz Waves* **2009**, *30*, 309–318. [CrossRef]
6. Yin, Y.; Wang, B.; Li, H.; Meng, L. Study of the relation between the surface loss and the field flatness in the EID. *Int. J. Electron.* **2017**, *104*, 204–217. [CrossRef]
7. Yin, Y.; He, W.; Zhang, L.; Yin, H.; Cross, A.W. Preliminary design and optimization of a G-band extended interaction oscillator based on a pseudospark-sourced electron beam. *Phys. Plasmas* **2015**, *22*, 073102. [CrossRef]
8. Booske, J.H.; Basten, M.A.; Kumbasar, A.H.; Antonsen, T.M.; Bidwell, S.W.; Carmel, Y.; Destler, W.W.; Granatstein, V.L.; Radack, D.J. Periodic Magnetic Focusing of Sheet Electron-beams. *Phys. Plasmas* **1994**, *1*, 1714–1720. [CrossRef]
9. Xie, J.; Zhang, L.; Yin, H.B.; He, W.L.; Ronald, K.; Phelps, A.D.R.; Chen, X.D.; Zhang, J.; Alfadhl, Y.; Yuan, X.S.; et al. Study of a 0.35 THz Extended Interaction Oscillator Driven by a Pseudospark-Sourced Sheet Electron Beam. *IEEE Trans. Electron Devices* **2020**, *67*, 652–658. [CrossRef]
10. Yin, Y.; He, W.; Zhang, L.; Yin, H.; Robertson, C.W.; Cross, A.W. Simulation and Experiments of a W-Band Extended Interaction Oscillator Based on a Pseudospark-Sourced Electron Beam. *IEEE Trans. Electron Devices* **2016**, *63*, 512–516. [CrossRef]
11. Li, H.-L.; Hu, C.-F.; Xu, C.; Yin, Y.; Wang, B.; Meng, L.; Wang, M.-Y. Plasma simulation to analyze velocity distribution characteristics of pseudospark-sourced electron beam. *Chin. Phys. B* **2020**, *29*, 105101. [CrossRef]
12. Cross, A.W.; Yin, H.; He, W.; Ronald, K.; Phelps, A.D.R.; Pitchford, L.C. Generation and application of pseudospark-sourced electron beams. *J. Phys. D-Appl. Phys.* **2007**, *40*, 1953–1956. [CrossRef]
13. Yin, H.; Cross, A.W.; He, W.; Phelps, A.D.R.; Ronald, K.; Bowes, D.; Robertson, C.W. Millimeter wave generation from a pseudospark-sourced electron beam. *Phys. Plasmas* **2009**, *16*, 063105. [CrossRef]
14. He, W.; Zhang, L.; Bowes, D.; Yin, H.; Ronald, K.; Phelps, A.D.R.; Cross, A.W. Generation of broadband terahertz radiation using a backward wave oscillator and pseudospark-sourced electron beam. *Appl. Phys. Lett.* **2015**, *107*, 133501. [CrossRef]
15. Yin, H.; Cross, A.W.; Phelps, A.D.R.; Zhu, D.; He, W.; Ronald, K. Propagation and post-acceleration of a pseudospark-sourced electron beam. *J. Appl. Phys.* **2002**, *91*, 5419–5422. [CrossRef]
16. Varun; Cross, A.W.; Ronald, K.; Pal, U.N. PIC Simulation of Pseudospark Discharge-Based Plasma Cathode Electron Source for the Generation of High Current Density and Energetic Electron Beam. *IEEE Trans. Electron Devices* **2020**, *67*, 1793–1796. [CrossRef]
17. Peng, R.; Bi, L.; Chang, Z.; Zeng, F.; Lin, M. Study of the oscillation startup time in a G-band EIO based on a pseudospark-sourced electron beam. In Proceedings of the 2017 Eighteenth International Vacuum Electronics Conference (IVEC), London, UK, 24–26 April 2017.

18. Shu, G.; He, W.; Zhang, L.; Yin, H.; Zhao, J.; Cross, A.W.; Phelps, A.D.R. Study of a 0.2-THz Extended Interaction Oscillator Driven by a Pseudospark-Sourced Sheet Electron Beam. *IEEE Trans. Electron Devices* **2016**, *63*, 4955–4960. [CrossRef]
19. Schuhmann, T.; Protz, J.; Fields, D.; Yin, H.; Cross, A.; He, W.; Bowes, D.; Ronald, K.; Phelps, A. A MEMS fabrication approach for a 200 GHz microklystron driven by a small-scaled pseudospark electron beam. In Proceedings of the Millimetre Wave and Terahertz Sensors and Technology III, Toulouse, France, 20–21 September 2010.
20. Yin, H.; Robb, G.R.M.; He, W.; Phelps, A.D.R.; Cross, A.W.; Ronald, K. Pseudospark-based electron beam and Cherenkov maser experiments. *Phys. Plasmas* **2000**, *7*, 5195–5205. [CrossRef]
21. Varun; Pal, U.N. PIC Simulation to Analyze Peak Electron Current Generation in a Triggered Pseudospark Discharge-Based Plasma Cathode Electron Source. *IEEE Trans. Electron Devices* **2018**, *65*, 1542–1549. [CrossRef]
22. Kumar, N.; Pal, U.N.; Verma, D.K.; Prajapati, J.; Kumar, M.; Meena, B.L.; Tyagi, M.S.; Srivastava, V. Experimental Analysis of Pseudospark Sourced Electron Beam. *J. Infrared Millim. Terahertz Waves* **2011**, *32*, 1415–1423. [CrossRef]